PERSPECTIVE

NJC
www.rsc.org/njc

Synthetic transition metal phyllosilicates and organic-inorganic related phases

Mireille Richard-Plouet,*[ab] Serge Vilminot[b] and Murielle Guillot[b]

[a] *Laboratoire de Chimie des Solides (CNRS UMR 6502), Institut des Matériaux Jean Rouxel, 2, rue de la Houssinière, BP 32229 44322 Nantes cedex, France. E-mail: Mireille.Richard@cnrs-imn.fr; Fax: +33 240 37 39 95; Tel: +33 240 37 39 96*

[b] *Groupe des Matériaux Inorganiques (CNRS-ULP UMR 7504), Institut de Physique et Chimie des Matériaux de Strasbourg, 23, rue du Loess, BP 43 67034 Strasbourg cedex 2, France. Fax: +33 388 10 72 47; Tel: +33 388 10 71 28*

Received (in Montpellier, France) 8th December 2003, Accepted 30th March 2004
First published as an Advance Article on the web 10th August 2004

We present a brief overview of the first-row transition metal phyllosilicates and their organically functionalised analogues obtained under autogenous pressure conditions. Some structural features of phyllosilicates are first recalled and the magnetic properties of Co^{2+} and Ni^{2+} phyllosilicates are described. In the second part, the state-of-the-art in organically functionalised phyllosilicates is reported, including our contributions on the structural and magnetic characterisation. The impetus is to enhance the potential of these new compounds as multi-property materials. Since our interest lies in low-dimensional magnetic properties, divalent transition metal cations are involved in the layered inorganic layers, whereas 3-aminopropyltriethoxysilane is used as the silicon source.

Introduction

For the past several years there has been a tremendous effort to synthesise organic-inorganic materials. The general goal is to couple two properties in a unique solid, one brought by the organic part and the other by the inorganic framework. One expects a synergistic effect between the two components, leading to original properties. Several examples can be presented, illustrating different approaches among the huge number of studies in this field. Some examples of organic-inorganic materials, synthetically obtained, are based on tetrachlorocuprate(II)[1] layered metal oxalate structures: (A)$_n^+$[$M^{II}M'^{III}(C_2O_4)_3$]$^-$. When A is a π-electron donor such as BEDT-TTF, magnetism due to the metal cation can be coupled

Mireille Richard-Plouet obtained her doctoral degree in 1994 at the Laboratoire de Chimie des Solides in the Institut des Matûriaux de Nantes (now Institut des Matûriaux Jean Rouxel) under the guidance of Luc Brohan. She joined the CNRS in 1995 and worked with Serge Vilminot at the Institut de Physique et Chimie des Matûriaux de Strasbourg. There, she developed the chemistry of transition metal phyllosilicates and studied their magnetic properties. She supervised the doctoral thesis of Murielle Guillot on organo-funtionalised phyllosilicates. In addition, she has studied the use of Eu^{3+} as a local luminescent probe in silicates and TEM on metal nanoparticles. In 2002, she returned to Nantes and rejoined Luc Brohanã s group and is now interested in the control of oxide poly-condensation.

Dr. Serge Vilminot received his PhD in 1975 at Montpellier University on work concerned with NLO and dielectric properties of organic–inorganic hybrid materials based on sulfates and fluoberyllates. He then turned to the study of fluorine ionic conduction in tin(II) derived fluorides like KSn_2F_5 or $PbSnF_4$. After moving to Strasbourg, he started activities in sol–gel science, mainly in the field of powder for ceramics. He also spent a significant amount of time on applied research. His present field of activities concerns the structure and magnetic studies of the hydroxysilicates and hydroxysulfates of transition metals.

Dr. Murielle Guillot obtained her PhD in Strasbourg in 2002. Her work focuses on the characterisation of organic–inorganic nickel silicates. She is currently working for OMYA, and is in charge of the scientific information and documentation at the Industrial Property department.

DOI: 10.1039/b316089k

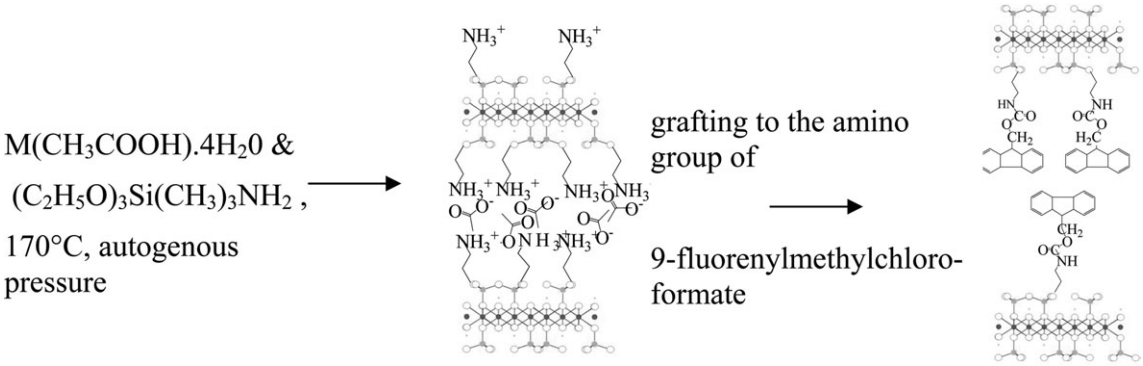

Scheme 1 Schematic view of the process used to obtain materials coupling low temperature magnetism and fluorescence. In a first step, a layered material, in which divalent transition metal cations are interacting, is synthesised. Secondly, grafting to the amino group is performed with an organic molecule.

to the conductivity property of the organic cation[2,3] Nonlinear optical behaviour can also be associated with such oxalate layers[4] or MPS_3 sheets[5] by introducing a polarisable, organic cation. In these cases, bonding between the two components is mainly ionic, through van der Waals interactions and/or hydrogen bonding. Ion-exchanged materials where ionic interactions between the organic and inorganic parts occurs, indeed lead to enhanced properties. For instance, the mechanical properties of polymers and their thermal stability can be improved by introducing a mineral component. This can be achieved starting from clays. One method is to disperse the silicate layers in a polymer matrix. An important step is devoted to the exfoliation of the starting mineral by a cationic precursor of the polymer,[6] where the polymer properties are greatly improved by the presence of the inorganic part.

Tailoring multi-property materials in which the organic part is covalently bonded to the inorganic layers remains an interesting challenge. One possibility is to graft, to a mineral layered structure, organosilanes, $RSi(OR')_3$. This allows one to introduce into the lamellar solid, the functionality of the R organic group, brought by the modified alkoxide. Different mineral phyllosilicates (layered silicates), such as montmorillonite, saponite or laponite, were successfully reacted with these organically modified alkoxides. These modified silicates can be applied to catalysis[7,8] or electroanalysis.[9] For instance, organo-modified intercalated laponite exhibits higher performance in enzyme entrapment. The controlled hydrolysis of 3-aminopropyltriethoxysilane leads to the formation of a cubic octamer that can also ion-exchange Na cations in natural montmorillonite.[10] Recently, instead of grafting to minerals, organically modified alkoxides were also used in one-pot synthesis leading to synthetic organo-modified phyllosilicates.[11–14] In this case, several applications can be considered, such as intermolecular reactions with guest species[15–17] or as absorption, in particular of heavy metals.[16,18]

Our primary aim concerns the evolution of the magnetic properties of materials with phyllosilicate and related structures. Keeping in mind the presence of a brucite-like layer ($M(OH)_2$) where the magnetic element can be introduced, one can tailor the magnetic interactions between these magnetic entities by tuning the nature of the organic species grafted to them and occupying the galleries. The first part of our work is devoted to the synthesis of transition metal phyllosilicates isostructural with their mineral counterparts and their characterisation, especially from the magnetic point of view. This work was necessary to understand the different behaviours we could expect from the magnetic layers. It was shown, in hydroxide structures that, depending on the interlayer distances, ordering from antiferromagnetic to ferromagnetic could be induced.[19] The second part deals with the synthesis of organo-modified phyllosilicates using solvothermal synthesis from organically modified silicon alkoxides and transition metal acetate and a description of the subsequent magnetic properties. These new structures can also be a source for more complicated materials by introducing, either by chemical reaction or by anion exchange, species exhibiting additional properties such as optical ones, for instance, and may provide possible interactions between magnetism and optics. Scheme 1 depicts the process carried out in our studies. Despite the low crystallinity of the obtained samples, our work also focuses on the possibility to get more insight into the structural model using the XAS (X-ray absorption spectroscopy) technique.

Transition metal phyllosilicates

Structural features of phyllosilicates

Prior to describing the experimental synthetic conditions for these materials, some structural features concerning phyllosilicates are reviewed.[20] This general term is used for silicates exhibiting a layered structure. As depicted in Fig. 1(a),[21] the structure is built up of sheets stacked along the *c* axis. They are built from brucite-type layers [$Mg(OH)_2$] where the divalent cation lies in octahedral sites sharing edges, covalently bonded to hexagonal rings formed by Si tetrahedron sharing their

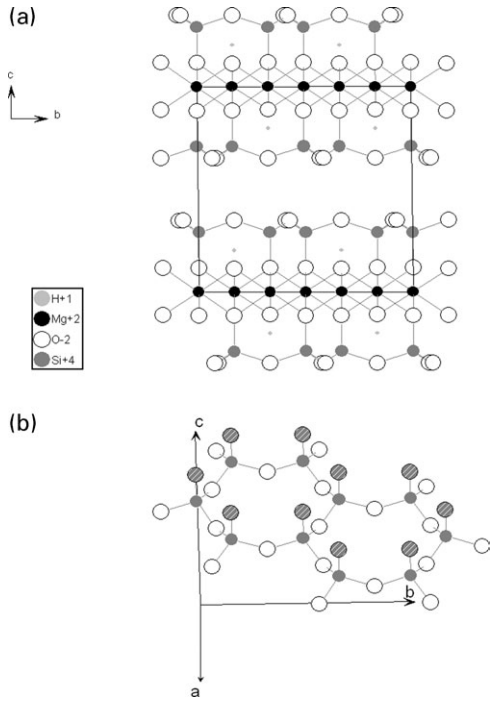

Fig. 1 (a) Projection along the *bc* plane of $Mg_3Si_4O_{10}(OH)_2$. (b) Representation indicating the connection between Si tetrahedra; hatched oxygen atoms are shared with the octahedral layer.

corners [Fig. 1(b)] at the surface. Two main structures can be built up corresponding to the following formulations: $M_3Si_2O_5(OH)_4$ and $M_3Si_4O_{10}(OH)_2$. The former exhibits only one Si layer connected to the octahedral layer and is thus named 1 : 1 phyllosilicate while in the latter, two Si layers sandwich the octahedral layer and the corresponding material is denoted as 2 : 1 phyllosilicate.

The silicon tetrahedra forming the hexagonal rings have a certain degree of flexibility and, therefore, can distort in order to accommodate the lattice difference between the octahedral and the tetrahedral layer. The size of the cation lying in the octahedral brucite sheet indeed directly defines the degree of agreement with the silica layer. Numerous divalent cations are found to occupy the octahedral layer in natural phyllosilicates, leading to more or less of a mismatch between both layered frameworks. In case it becomes too important, distorting the silica ring and/or the hydroxide layer is not enough and several extended defects can take place such as bending of the sheets, puckering of the layers or intergrowths.

From these ideal compositions, depending on the elements present during the formation of the silicate, different situations can occur. For instance, the three divalent cations can be replaced by two trivalent cations and then a vacancy is created in the octahedral sheet. This leads to dioctahedral phyllosilicates compared to trioctahedral ones when all the sites are occupied. In these two latter situations, the sheets are neutral and held by van der Waals interactions. It is possible to induce a negative charge in the sheets either by substituting Si^{4+} by Al^{3+} or by creating vacancies in the octahedral layer. A counter cation lies then in the gallery for charge balance. Alkalis or alkaline earths are mainly encountered in clays. Some typical characteristics of the X-ray diffraction pattern can be summed up as follows. Phyllosilicates crystallise in the monoclinic or triclinic system with unit cell parameters as depicted in Fig. 1 (triclinic cell, with $a = 5.290$, $b = 5.173$, $c = 9.460$ Å, $\alpha = 90.46°$, $\beta = 98.68°$, $\gamma = 90.09°$). The interlayer distance is close to 7 Å for 1 : 1 phyllosilicates while it is 9.4 Å for 2 : 1 phyllosilicates and can reach 15 Å for hydrated clays and even more when voluminous organic molecules are inserted between the layers. This generally gives rise to a progression of (00ℓ) reflections at low angles in the X-ray diffractogram. Two other Bragg peaks are generally observed corresponding to (hk0) indexations: one close to 2.55 Å corresponding to (130) or (200) and the other close to 1.55 Å corresponding to (060) or (330). These two peaks also appear for divalent cation hydroxides crystallising with a brucite arrangement and are related to (100) and (110) diffraction planes for the 2.55 and 1.55 Å lines, respectively. Since they mainly involve the octahedral layer, their positions are very sensitive to the proportion of vacancies in the layer. For instance, the (060/330) reflection is shifted to 1.50 Å for dioctahedral phyllosilicates.

Phyllosilicates substituted by magnetic divalent cations

In order to construct magnetic organic-inorganic frameworks based on these materials, the first step of our work was devoted to the synthesis of phyllosilicates of nickel and cobalt and the characterisation of their low temperature magnetic properties. The synthesis is performed under autogenous pressure with or without fluoride as a mineralising agent. This procedure is carried out in order to obtain clay or related materials.[22] In our case, we proceed from $M^{II}(CH_3COO)_2 \cdot 4H_2O$ and tetraethylorthosilicate [$Si(OC_2H_5)_4$]. The alkoxide is hydrolysed and condensed to a gel, then dried at 100 °C. The solid is ground and dispersed in an acetate solution. The suspension is heated at 220 °C for several days. Different phyllosilicates corresponding to $M_3Si_2O_5(OH,F)_4$ and to $M_3Si_4O_{10}(OH,F)_2$ with M = Co[23] or Ni[24] have been isolated.

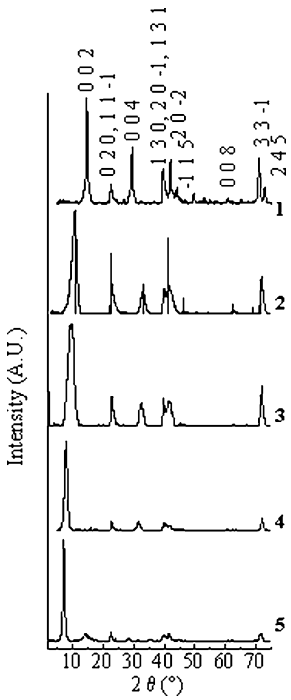

Fig. 2 X-Ray diffraction patterns of Co phyllosilicates obtained under hydrothermal conditions. Reprinted from ref. 23 with permission from Elsevier (copyright 1999).

These materials are isostructural and similar to the mineral compounds, namely 1 : 1 or 2 : 1 phyllosilicates. The interlayer distance ranges from 7 Å for 1 : 1 phyllosilicates to 9.4 Å for 2 : 1 phyllosilicates (Fig. 2). The characteristic features of the X-ray diffraction diagram can be summed up as intense (00ℓ) reflections (at low thetas) together with (hk0) reflections located at 2.55 and 1.55 Å. The solids we obtained present relatively broad (00ℓ) reflections, indicating a low degree of crystalline coherence along the stacking axis. Indeed, when observed by transmission electron microscopy, the crystals appear as very thin platelets, as depicted in Fig. 3. Lateral dimensions in the nanometer range allow us to qualify these objects as nanocrystals.

Due to their rather low crystallinity, techniques providing information on the local environment, such as X-ray absorption spectroscopy (XAS), were undertaken.[25] Probing around

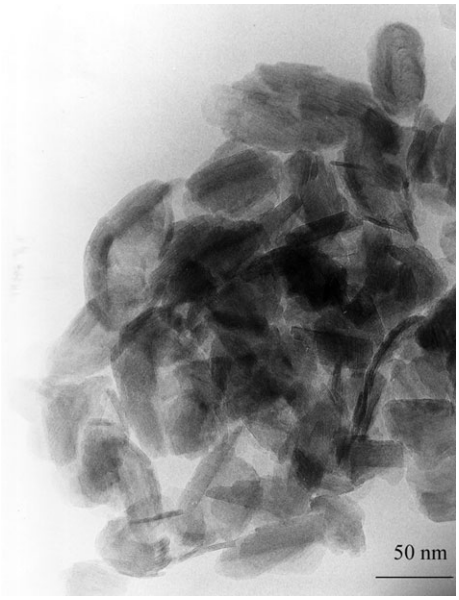

Fig. 3 Transmission electron microscopy of a Ni 1 : 1 phyllosilicate.

the metal cations confirms that the first neighbour shell consists of 6 oxygen atoms at 2.04(5) Å and the second shell has 6 M cations located at 3.06(5) Å. These distances are consistent with the occurrence of a hydroxide-like layer. However, to fit the experimental data it was necessary to take into account the presence of a third shell. Thus, 2 silicon atoms were introduced in the local environment at a distance of 3.24(5) Å, in agreement with the presence of Si tetrahedra grafted to the layer as in phyllosilicates.

In order to tune the interlayer distance several approaches were carried out. The first approach is based on acid-base exchange starting from a synthetic clay framework. The idea is to create negatively charged sheets either through substitution of Si^{4+} by Al^{3+} or by varying the stoichiometry, inducing the formation of vacancies on the octahedral layer. The latter situation is currently observed in minerals leading to dioctahedral phyllosilicates, only 2/3 of the octahedral sites are thus occupied. The charge balance is assumed by a counter-cation lying in the interlayer spacing, namely an alkali. The latter can be exchanged in acid solution by proton or directly by an alkylammonium ion as already successful performed for other layered structures.[26] Such a "chimie douce" process induces deterioration of the crystallinity upon sequential insertions. This is contrary to expectations for characterising the solids during the different steps of the process. Moreover, even if tuning of the charge through Al substitution could be achieved, magnetic measurements revealed that some of the Al is also substituted for the transition metal cation in the octahedral positions.[23] Magnetic properties are not comparable between samples with totally occupied sites and partially occupied ones. Another approach consists in using amines, which are expected to lie in the gallery. This was attempted with propyl-, butyl-[27] and triethylamine and allows one to increase the interlayer distance up to 14.3 Å.[23]

All these compounds present a paramagnetic-ferromagnetic transition at low temperature. Above 100 K, susceptibility measurements follow a Curie–Weiss law [$\chi = C/(T-\theta)$, with $C = Ng^2\mu_B^2 s(s+1)/3k$, considering a spin-only equation]. The Landé factors are in agreement with the values obtained for Co^{2+} and Ni^{2+} in octahedral sites, 2.2 and 2.6, respectively. The ordering temperature is different when Co or Ni cations are involved in the structure with T_c close to 15 and 27 K, respectively. Especially in the case of Co, the transition is broad, probably due to pre-transitional effects. Indeed, when approaching the transition, the correlation length of the magnetic moments increases gradually until enough moments are coupled to induce the transition towards a 3D ferromagnetic order in the material. It has to be pointed out that the geometry observed in the solid is quite favourable to a ferromagnetic coupling between neighbouring metal cations. Indeed, the d orbitals of the transition metal are interacting through the p orbitals of bridging oxygens *via* a superexchange interaction.[28] The coercive fields measured at 2 K are close to several thousands for Ni compounds while there is almost no coercivity for Co phyllosilicates. For the former, it was possible to show that the easy magnetisation axis is perpendicular to the layers whereas the anisotropy appears less marked for Co compounds. This result is surprising since the Co^{2+} cation is expected to be more anisotropic. No correlation could be pointed out between magnetic ordering (transition temperature or nature of the coupling between layers) and the distance between layers. In this system, the intralayer magnetic moments are coupled ferromagnetically *via* superexchange through the oxygen atoms. More and more moments are coupled when approaching T_c until the interlayer ferromagnetic coupling takes place. Once the magnetic behaviour of this system has been studied, it is possible to play with this framework in order to introduce, if possible, another property. Using an organo-modified alkoxide is a smart way to achieve this goal.

Organically modified synthetic phyllosilicates

Synthesis, reactivity and characterisation of organic-inorganic phyllosilicates, obtained by precipitation

If some studies have been reported, starting from a cation salt and an organo-modified silicon alkoxide, none have dealt with their magnetic properties. The first reported set of experiments was conducted in water–methanol with Mg and Ni chloride hexahydrate and 3-methacryloxypropyltrimethoxysilane [$H_2C{=}CHCH_3{-}CO{-}O(CH_2)_3\,Si(OCH_3)$] precipitated by sodium hydroxide.[11,12] Other alkoxides have also been used (summarised in Table 1).[29–37] The synthesis procedure varies slightly in the different reports. It can be performed in water–methanol or water–ethanol mixtures, in the presence of sodium hydroxide, at room temperature with ageing for 24 h. In addition to such processes, da Fonseca *et al.* also used the following

Table 1 Organo-modified alkoxides used for the synthesis of modified phyllosilicates and the interlayer spacing of the resulting materials

R in $RSi(OCH_3)_3$ or $RSi(OC_2H_5)_3$	M	d_{001}/Å	pH	Reference
Methacryloxypropyl	Al	20.31	5.5	14
	Mg	18		11
		19.62	9	12
		16.93	11.5	14
		14.8		15
	Mg, Li	15.1	8.5–9	33
	Ni	18		11
		16.98	9	12
		13.80	13	12
Methyl	Mg	8.9		15
Isobutyl	Al	19.80	5.5	14
	Mg	11.45	11.5	14
Octyl	Al	24.95	5.5	14
	Mg	20.16	11.5	14
	$Mg_{1.7}$,	25.1		36
	$Al_{1.5}$	17–20.8		37
Pentyl	Al	22.20	5.5	14
Dodecyl	Al	37.98	5.5	14
	Mg	24.24	11.5	14
Phenyl	Al	16.96	5.5	14
	Mg	11.83	11.5	14
		11.8		15
	Mg, Li	13.0	8.5–9	33
3-Mercaptopropyl	Mg	13.0		15
		13		30, 31
		12.1		32
	Cu	6.95		31
3-Aminopropyl	Mg	18.6		15
		17.3		18, 29
		13.5		35
	Ni	13.6 (RT)		17
		16.4 (50 °C)		17
Glycidylpropyl	Ni	17.5		13
	Mg	15.9		16
3-(2-Aminoethyl-3-aminopropyl)	Mg	15.3	12	16
		18.5	7	16
		20.53		18, 29
	Ni	19.6 (RT)		17
		21.5 (50 °C)		17
1-Propenyl	Mg	11.1		16
Dihydrotriethoxysilyl-propyl-1*H*-imidazole	Mg	13.2		16
Propyl diethylenetriamine	Mg	23.23		29
	Ni	24.5 (50 °C)		17
3-Acryloxypropyl	Mg, Li			33
3-Propylurea	Mg	23		34
3-Pentylurea	Mg	25		34
3-Heptylurea	Mg	27		34

procedure: mixing of the reactants at 100 °C before the suspension is aged at 50 °C for 5 days.

Magnesium silicates have mainly been synthesised whereas some studies are devoted to Al,[14] Ni or Cu compounds. The role of the pH due to NaOH as precipitant is mentioned for 3-aminopropyl- and 3-(2-aminoethyl-3-aminopropyl)triethoxysilane. When the reaction is performed under alkaline pH, the amino group is not protonated whereas it is at neutral pH, inducing the presence in the gallery of Cl^- anion coming from the reactant. Modified hectorite is obtained under reflux in water for 2–5 days in the presence of LiF, in order to obtain $[Li_{0.66}(Mg_{5.34}Li_{0.66})Si_8O_{12}R_8 \cdot xH_2O]$.[33] It seems that this condition partly induces hydrolysis of the Si–C bond. If starting from a divalent cation induces the formation of trioctahedral layers, introducing Al^{3+} cations alone or in substitution for Mg^{2+} ions tends to promote the formation of dioctahedral slabs.[14,37] More recently, a synthesis under autogenous conditions at 200 °C was reported, starting from octadecyldimethyl(3-trimethoxysilylpropyl)ammonium chloride (ODAC) and silica sol mixture together with magnesium hydroxide.[38]

Organo-modified phyllosilicates present interlayer distances ranging from 11 to 38 Å, depending on the organic group bonded to Si. Only the (001) reflections are observed except for Al based materials obtained at pH = 5.5, for which higher order reflections are visible. The d_{001} distance is consistent with an interpenetrating arrangement of R groups, with again Al dioctahedral materials being the exception, for which a bilayer chain arrangement occurs. A broad hump close to 4.5 Å is indexed as the (020/110) reflections. Other in-plane reflections are generally identified: (130/200) at 2.55 Å and (060/330) at 1.55 Å.[11–18]

These processes lead to poorly crystallised solids, which appear difficult to characterise. The commonly admitted hypothesis concerning the structure of these organo-modified phyllosilicates is to classify them as phyllosilicates with an enhanced interlayer distance due to the presence of the organic species connected to the silicon atoms.

Whatever the mineral considered, it has to be noted that in the hexagonal silica ring all oxygen atoms of the tetrahedra are bridging. This is possible with oxygen atoms but becomes doubtful when a Si–C bond is present. Attempts to obtain experimental data concerning the connectivity of the Si framework were made using NMR techniques. Generally, three kinds of connectivities between Si atoms are observed, namely T^1, T^2 and T^3 species corresponding to R–Si–[O(M/Si)]–$(OH)_2$, R–Si–$[O(M/Si)]_2$–OH and R–Si–$[O(M/Si)]_3$, respectively. The materials give rise to broad peaks, indicating that Si tetrahedra are in their majority condensed, especially when syntheses are performed at neutral pH. No information on the occurrence of a M–O–Si bond could be obtained. Generally, it is admitted that the silicon part is connected to the layer and is present as small oligomers.

Two mechanisms are invoked to explain the formation of these phases at room temperature. The first one is based on the coupling of partially condensed organo-modified alkoxysilanes on the brucite layer and is favoured at high pH. For alkoxides involving amino groups, no T^3 {R–Si–$[O(M/Si)]_3$} species are observed in the solid obtained with aminopropyltriethoxysilane in methanol or with aminoethylaminopropyltriethoxysilane in alkaline pH.[16,15] The extension of the in-plane organisation is governed by the condensation degree of the alkoxide relative to the formation of the hydroxide layer. Hydrolysis of alkoxide is known to slow down under alkaline conditions relative to condensation, whereas formation of the hydroxide is favoured. Under these conditions, the uncondensed silicate species are rapidly grafted to brucite layers since Si–O–Mg and Mg–O–Mg bond formation are promoted. At lower pH, a higher degree of condensation can occur before bonding to the inorganic hydroxide framework. This explains why the degree of condensation of the Si tetrahedron is higher for samples obtained at neutral rather than under alkaline conditions. In any case, condensation of the alkoxide is generally not totally achieved prior to its incorporation into the solid. The other mechanism invoked for the formation of these layered compounds involves a cooperative assembly between the hydrophobic organic, partially condensed alkoxide part and the inorganic brucite layers, as involved in mesoporous silica synthesis.[14,16] This was in particular smartly established for Al based compounds, for which the degree of order between slabs is directly correlated to the length of the organic group.[14] As suggested by the authors, preparation of the Al materials is performed at rather acid pH (5.5), which is in favour of rapid hydrolysis of the alkoxides prior to their condensation. This condition can promote lamellar ordering by surfactant interactions with hydrophobic organic groups and hydrophilic silanol groups. A further condensation step leads to a negatively charged layer in the surfactant part, attracting the Al species, which condense to form the inorganic layer.

Several studies indeed report the accessibility of the organic group. The first reported example involves the reaction of a glucidoxypropyl modified nickel phyllosilicate, with a macrocyclic ligand: 1,12-diaza-3,4:9,10-dibenzo-5,8-dioxacyclopentadecane.[13] Binding constants for Co^{2+}, Ni^{2+}, Cu^{2+} and Zn^{2+} cations were determined. Gold nanoparticles were formed by reacting $AuCl^-_4$ with mercaptopropyl modified phyllosilicate.[15] Moreover, it has been shown that *in situ* reactivity can take place: (1) *via* cross linking of the epoxide group by dry thermal heating in the presence of *m*-phenylenediamine; (2) by a ring-opening reaction in the presence of methyl thioglycolate, both processes inducing disorder between the layers[16] and (3) *via* reaction between amino groups and 2-pyridinecarboxaldehyde, inducing creation of a C=N bond by water elimination.[31]

These materials were also studied as absorption matrices for heavy metal cations. Phyllosilicates obtained from amino- and mercapto-modified alkoxides were contacted with transition metal cations, Co^{2+}, Ni^{2+}, Cu^{2+} and Zn^{2+}, or heavy metal ions, Hg^{2+}, Pb^{2+} and Cd^{2+},[32] in solution. The latter study demonstrated that a Mg phyllosilicate including mercapto groups exhibits high metal ion uptake capacities and an equivalent affinity for the three heavy metal cations. Moreover, an acid treatment allows one to recover the material without altering its absorption capability. In the former study, metal uptake seems to be accompanied by chemical reaction between the initial amino or diamino layered material, leading to an increase of the interlayer distance for Co^{2+} and to recrystallisation for Cu^{2+}, Zn^{2+} and Ni^{2+} cation uptake.[18] The possibility to form a complex with the N atom in the interlayer spacing is evoked, together with the slabs being brought closer to satisfy the M–N distances in the complex. The final materials present an interlayer distance close to 7 Å as for 1 : 1 phyllosilicates. Starting with mercaptopropyl phyllosilicate,[30,31] Zn and Cu uptake also induce recrystallisation into new structures, namely a sauconite-like solid for Zn (2 : 1 phyllosilicate with Al^{3+} in the layer and $0.3 \cdot Na^+$ counter cation as charge balance, with a 15 Å interlayer distance) and a 1 : 1 phyllosilicate for the Cu treated solid. Batches with Ni or Co lead to amorphous solids by X-ray diffraction. No attempts to regenerate the precursor were mentioned.

Shortly after these works appeared, we also had considered the possibility to obtain organic-inorganic phyllosilicates by using as the silicon source an organically modified alkoxide and subsequently treating the reactants under autogenous pressure conditions.

Organic-inorganic transition metal silicates, obtained under autogenous pressure conditions

Among the several alkoxides we have tested [typically 3-(2-aminoethyl-3-aminopropyl)triethoxysilane, octyltriethoxysilane] we finally focused our studies on 3-aminopropyltriethoxysilane

or APTES. This reagent is used in different fields as a coupling agent in the treatment of glass fibres or more generally as a chemical modifier of silica or alumina surfaces.[39] Contrary to the reported studies, the alkoxide is used as received but is stored under dried Ar, to avoid hydrolysis. It is added dropwise into the transition metal ($M = Ni^{2+}$ or Co^{2+}) acetate solution, under stirring. The suspension is introduced into an autoclave and heated at 170 °C, in order to enhance crystallinity. This temperature is optimised and prevents decomposition of the amino group. Particular attention is paid to the influence of different parameters on the final compound such as concentration of reactants, duration of synthesis, presence of F^- anions coming from HF or NH_4F, pH of the initial suspension, especially for Ni compounds.[40] Contrary to the experiments described in the literature, methanol was avoided in our work because 3-aminopropyltriethoxysilane tends to form an octamer [$(RSiO_{3/2})_8$, $R = (CH_2)_3NH_2$] in its presence.[41]

Concerning Ni silicates, at least three phases could be identified. At pH greater than the pK_a of aminopropyl (close to 10[42]) the amine is not protonated and the interlayer distance is close to 15.4 Å as determined by X-ray diffraction data. From chemical analysis, this phase exists for Ni : Si close to 3 : (2.6–2.9). It also has to be pointed out that such basic pH leads to the degradation of the amino group, since in the solid, half of the nitrogen is missing when compared to the Si content. As already proposed in the literature, under these conditions, the formation of the hydroxide layers takes place together with hydrolysis and condensation of the alkoxide.[15] The latter process inhibits the development of the layered framework, leading to less crystallised materials. At pH below 10, two phases can be obtained, depending on the water quantity. At low concentration, the analysis of the silicate leads to a Ni : Si ratio equal 3 : 1 while in more concentrated conditions, the Ni : Si ratio reaches a value of 3 : 2.[43] The degradation of the amino group is no longer observed under these conditions, since chemical analysis reveals quite similar values for the Si and N contents. For both compounds, carbon is always found in excess and the presence of acetate anions has been considered in order to interpret this. Therefore, IR and Raman spectroscopies confirm that the amine group is protonated and specific vibration bands of acetate anions are observed.

From the X-ray diffraction (Fig. 4), both compounds appear as layered materials with the characteristic features attributed to phyllosilicates, except that the interlayer distance is larger at 21.1 Å. The introduction of the amino group seems to enhance the crystallinity when the synthesis is performed in more dilute conditions. When compared with phyllosilicates, the enhancement is noteworthy. For these compounds, the (00ℓ) reflections

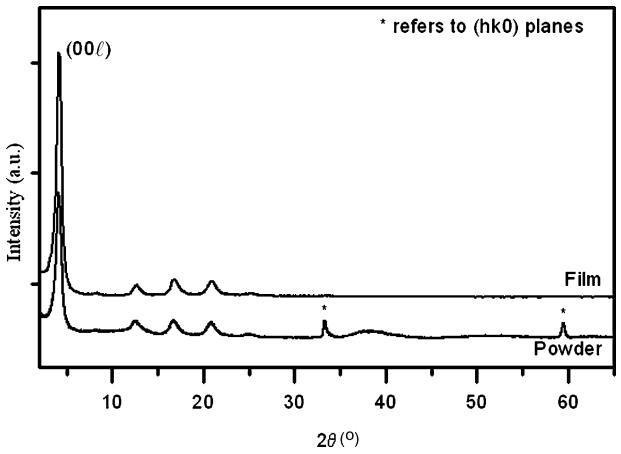

Fig. 4 X-Ray diffraction patterns of Ni phyllosilicate obtained in diluted conditions, reprinted from ref. 25. Reproduced by permission of The Royal Society of Chemistry.

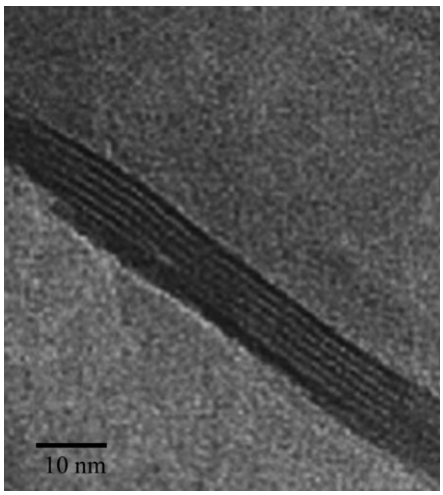

Fig. 5 Transmission electron microscopy image of a lamellar crystal of an Ni aminopropyl silicate (Ni/Si = 3/2), embedded in an epoxy resin, reprinted from ref. 25. Reproduced by permission of The Royal Society of Chemistry.

are broad due to the slight thickness of the crystallites along the stacking axis (Fig. 4). The main difference between both compounds, except for the Ni : Si ratio, lies in the number of coherently stacked slabs along the stacking axis. For Ni : Si = 3 : 2, the coherence length estimated from the Scherrer relation is 7 nm whereas it is 11 nm for Ni : Si = 3 : 1. This low coherence is confirmed by TEM observations performed on an orientated preparation embedded in an epoxy resin and cut perpendicularly to the obtained film (Fig. 5).

The low quality of the diffractogram does not allow one to refine a structural model, therefore X-ray absorption spectroscopy was undertaken in order to check the grafting of the silica species to the hydroxide layers. (NMR spectroscopy was time-consuming and not conclusive due to the presence of paramagnetic Ni^{2+} in the close neighbourhood of the Si atoms.) Analysis of the XAS spectra performed on powders confirms the first oxygen shell around Ni with N oxygen atoms located at 2.05(5) Å, and the second shell with N Ni at 3.11(5) Å. As for phyllosilicates, taking into account a third shell with Si atoms at 3.24(5) Å greatly increases the fit quality.[25] Several authors working on the synthesis of such materials but mainly concerned with Mg claim that Si tetrahedra are arranged as in phyllosilicates. This structure is doubtful since in this case every oxygen atom is shared with other tetrahedra or with the hydroxide layer. Such a geometry cannot occur when one of the tetrahedron edges is a carbon atom belonging to the amino chain. No experimental information is available to support the hypothesis that the structure of this material is indeed analogous to the minerals.

The ability of our samples to give rise to highly oriented thick tapes on a substrate has been exploited to perform polarised EXAFS.[44] This technique was successfully used by Manceau and collaborators on films obtained by settling of clays.[45] It is necessary to use oriented films with a majority of the crystals set with the c^* axis perpendicular to the substrate. Nickel silicates were dispersed in water, forming a stable colloidal solution and allowed to settle on different substrates by slow evaporation of the solvent. X-Ray diffraction confirms the preferential orientation of the crystallites: only the (00ℓ) reflections are observed (Fig. 4). This indicates that the crystals lie on the substrate with the stacking axis perpendicular to the substrate.

Quantitative texture analysis (QTA) of the films, deposited on glass slides, was performed in collaboration with Chateigner. In Fig. 6 are presented the experimental and complete normalised calculated pole figures, together with the low-index

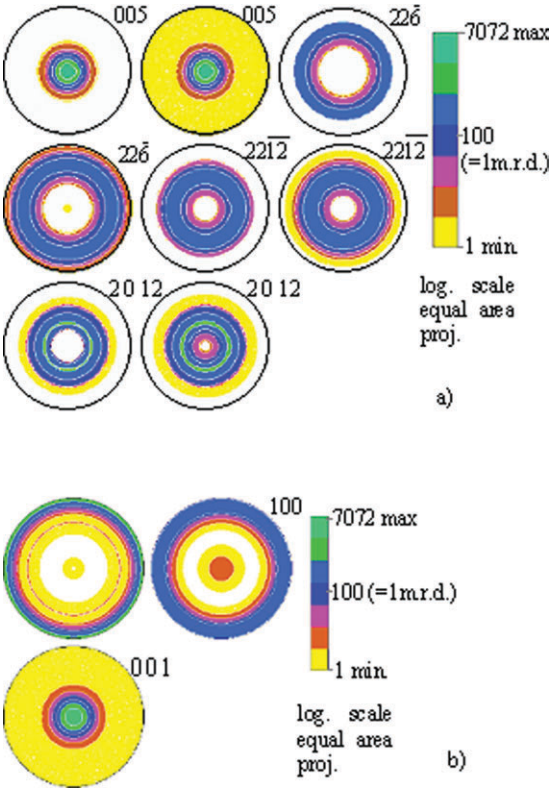

Fig. 6 (a) Experimental-normalised pole figures and complete recalculated normalised pole figures for the Ni : Si = 3 : 1 sample. Logarithmic density scale and equal area projections are used. Reprinted from ref. 44 with permission from Elsevier (copyright 2003). (b) Low-index figure pole recalculated, indicating the anisotropy of the c^* distribution.

pole figures for simple directions: {100}, {010} and {001}. The experiments revealed that the silicate obtained in the lowest solution concentration presents a strong texture characterised by a maximum density value close to 71 m.r.d. (multiple random density) in the fibre direction and a relatively sharp distribution of the crystallites relative to the film substrate. Thus, the full width at half maximum (ψ) is only 15.4°, using a Gaussian model, whereas it is 38.6° for the silicate obtained in a more concentrated solution (Fig. 7). It is noteworthy that the sample with Ni : Si = 3 : 1 is strongly oriented when compared to other clay materials.

The high quality of the textures, quite comparable with those obtained for already studied clays, allows us to characterise them by polarised EXAFS (P-EXAFS). The principle is to probe selectively around an absorber by rotating the sample

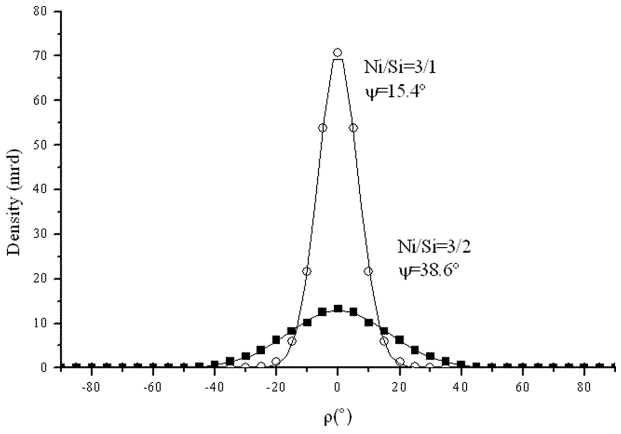

Fig. 7 Dispersion curves of the {001} pole figures for the organo-modified Ni phyllosilicates. Reprinted from ref. 44.

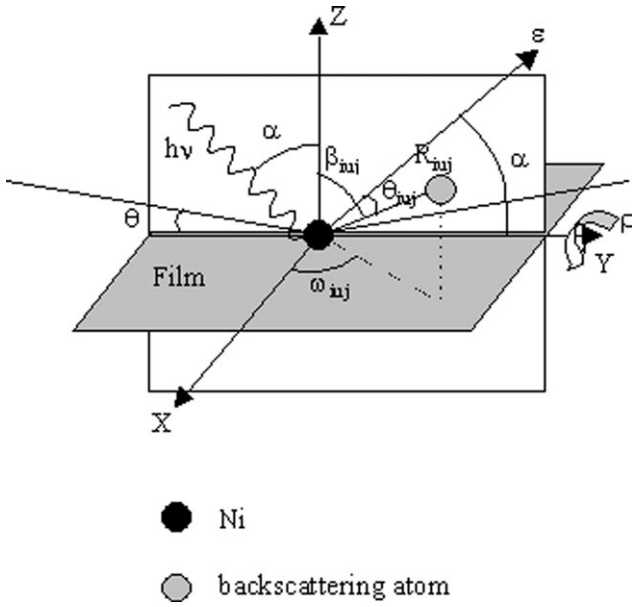

Fig. 8 Coordinate system for angular measurements on self-supported film. Reprinted from ref. 44.

with respect to the incident linearly polarised synchrotron beam. When the incident beam is perpendicular to the film, the electric field is parallel to the film and to the sheets of the silicate, so that the "in-plane" atoms are mainly probed whereas when the X-ray beam is parallel to the film, the information comes from the "out-of-plane" atoms (Fig. 8). In fact, the latter geometry cannot be reached experimentally but the absorption coefficient, $\chi(\alpha)$, can be calculated from several absorption coefficients obtained for different angles between the normal to the film and the beam (α). The angular dependence can be written as eqn. (1)[46] for each value of k:

$$\chi(\alpha) = \chi(90^\circ) + [\chi(0^\circ) - \chi(90^\circ)]\cos^2\alpha \quad (1)$$

Manceau and co-workers have shown that it is possible to evaluate the angle β_{iuj} between the c^* direction and the direction defined by the absorber-backscatter atoms (Fig. 8). For phyllosilicates, this angle is close to 60° for the oxygen atoms in the first shell, close to 90° for M cations in the second shell and in the 22–40° range for Si atoms in the third shell.[20] By plotting the coordination number, N_j^{app}, for each neighbour j *versus* $\cos^2\alpha$, a linear dependence is expected, according to eqn. (2):[47]

$$N_j^{app} = N_j^{real}(1 - I_{ord} + 3I_{ord}\cos^2\beta) - \tfrac{3}{2}N_j^{real}I_{ord}(3\cos^2\beta - 1)\cos^2\alpha \quad (2)$$

where N_j^{app} and N_j^{real} correspond to the number of j atoms around the Ni atoms, for each signal and the real coordination, respectively. The former is calculated by fitting signals corresponding to each shell; the latter is evaluated by using eqn. (2). In the coefficients of the linear regression appear the angle β. When β is greater than 54.7°, the slope is positive. Therefore, as in the case of phyllosilicates, this slope is negative for N_{Si}^{app} *versus* $\cos^2\alpha$ since β_{Si} is smaller than 54.7°.

Another parameter, I_{ord}, related to the texture of the film, has to be determined prior to performing P-EXAFS. This parameter accounts for the particle disorder. Its value is 1 for a single crystal and decreases as the order also decreases, reaching 0 for a powder. The ψ values allow us to determine I_{ord} to 0.82 and 0.96, respectively, for Ni : Si = 3 : 2 and Ni : Si = 3 : 1 compounds by using ref. 48. A strong dependence of the absorption coefficient on the angle α can be pointed out. The $\chi(90^\circ)$ spectrum is calculated and the linear regression [see eqn. (1)] is checked for each k value. Then, for each shell, O, Ni and Si neighbours, the fitted coordination is plotted against $\cos^2\alpha$. A linear regression is observed and β_O, β_{Ni} and β_{Si} are

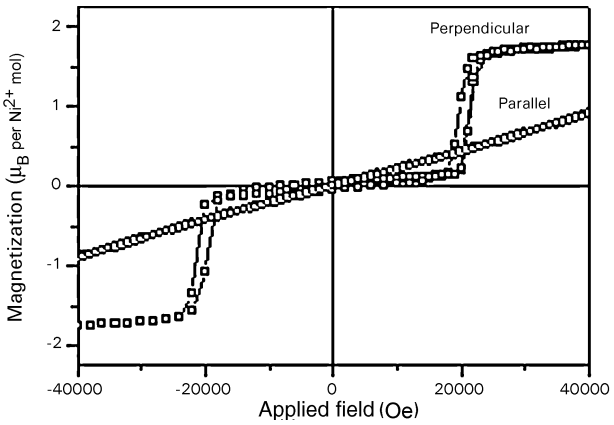

Fig. 9 Magnetisation *versus* applied field at 2 K, field perpendicular and parallel to the surface of a self-supported film. Reprinted with permission from ref. 43. Copyright (2002) American Chemical Society.

evaluated. As far as oxygen and nickel atoms are concerned, the angles are rather in agreement with the expected ones. For Si atoms, β angles are in the 60–62° range and far from the value reported for phyllosilicates (22–40°), indicating that the structure is different from the hexagonal ring arrangement found in these minerals. But several remarks have to be made. First of all, despite the texture, it is necessary to introduce Si atoms around the Ni, even for $\alpha = 0°$; this means that the information mainly comes from the "in-plane" atoms. This indicates that for every orientation, Si is present and not only perpendicularly to the layer. This can be related to the nanocrystalline nature of the materials. The Si atoms located in the inner part of the crystals are grafted to the layers with a small β angle, explaining the observed interlayer distance. Those located at the edges are less constrained and in order to avoid steric hindrance, they can be connected parallel to the layer and induce a large β angle. If taking into account the Si around Ni in a third shell improves the fit, it has to be remembered that this contribution is greatly hidden by the contribution of the 6 Ni atoms present at close range.

The experiment was conducted for Ni silicates with Ni : Si = 3 : 2 and Ni : Si = 3 : 1. There is no difference locally around the Ni atoms between both samples. But they exhibit different phases and in particular, different low temperature magnetic ordering. The former orders ferromagnetically below 18 K[24] as for the previously studied Ni phyllosilicates while the latter presents a transition towards a canted antiferromagnetic ordering at 21 K.[43] The associated events in the a.c. susceptibility are very sharp with a contribution to the imaginary component. The magnetisation *versus* applied field at 2 K presents a 2 T critical field beyond which magnetisation abruptly increases until saturation is reached at 5 T. When decreasing the applied field a slight hysteresis appears with a remnant magnetisation, giving an estimate of the canting angle of 0.8°. Experiments performed on self-supported oriented samples indicate that there is a strong magnetic anisotropy with the easy axis perpendicular to the layers (Fig. 9). This original behaviour has been interpreted on the basis of ferromagnetically coupled moments inside the layers interacting antiferromagnetically from one layer to the other at low temperature without applied field. A spin-flop-type transition is induced when increasing the applied field. This particular

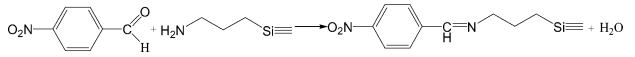

Scheme 2 Grafting between *p*-nitrobenzaldehyde and aminopropyl group of the silicon alkoxide by formation of an imine.

behaviour can only be related to the difference in crystallinity between both silicates. An exchange path can occur *via* hydrogen bonds between layers in an easier way since there is less disorder in the "antiferromagnetic" compound.

Cobalt organo-modified silicates could also be obtained, leading to lamellar compounds as well with an interlayer distance close to 18 Å. Upon reaction with ethanol the latter can be increased to 21.4 Å. Varying the concentration of the reactants in the autoclave does not allow, as in the Ni case, to tune the magnetic properties since all the compounds we measure become ferromagnets at low temperature, with T_c close to 5 K.

The possibility to react organic molecules with the ammonium group of the organo-modified alkoxide was tested. Two organic functions were selected: an aldehyde and an acyl chloride. *p*-Nitrobenzaldehyde was already successfully grafted to 3-aminopropyltriethoxysilane[49] used as a binding agent on Si wafers. A solution of the aldehyde was refluxed at 60 °C in ethanol together with a suspension of silicate in the presence of molecular sieves in order to retrieve water molecules formed during the reaction.[25] The reaction implies the formation of an imine according to Scheme 2. The system absorbs in the UV range. Moreover, nonlinear optical properties could be expected due to the NO_2 group, which allows polarisation of the molecule under an electric field.

Another molecule, 9-fluorenylmethylchloroformate (FMOC), was chosen because it is fluorescent and used to reveal a low content of amino acids. The reaction (Scheme 3) in a water–dioxane mixture at 0 °C together with Na_2CO_3 in order to neutralise HCl, formed as a by-product, gives rise to a carbamate.[40] After filtration and washing with the solvent used during the reaction, the solids present diffractograms characteristic of organo-silicates with an increased interlayer distance. From a value of 21.1 Å for the preliminary compound the d_{001} reflection reaches 22.7 and 30.9 Å for the imine and carbamate solids, respectively. By comparison with the initial material, it is noteworthy that the crystallinity of the sample is maintained during the process. IR spectroscopy indicates that the characteristic vibrational bands of the organic species are superimposed onto the bands of the inorganic framework and that the acetate anions disappear during the reaction. The latter consideration is related to the following equilibrium: $Si–R–NH_3^{+}{}^{-}OOCCH_3 \rightleftharpoons Si–R–NH_2 + CH_3COOH$, which is shifted toward the right side when the solid is dispersed in a solvent less polar than water. Thus, the amino group is no longer protonated since the reactions proceed by attack on the nitrogen doublet; grafting can take place, together with acetic acid release in the solvent. As soon as this reaction begins, the equilibrium tends to displace towards the right side. In the resulting compound, the layers are no longer charged and the solid part settles in the beaker. No change in the magnetic characteristics was brought to the fore when modifying the interlayer function.

In order to check the possible exchange of acetate anions with other anions, a nickel silicate was dispersed in water

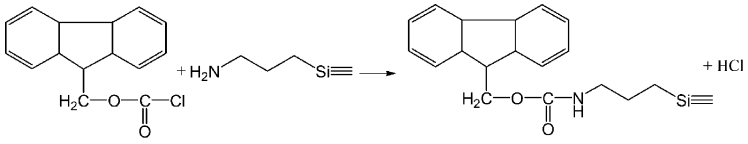

Scheme 3 Carbamate formation by reaction between 9-fluorenylmethylchloroformate and aminopropyl group of the silicon alkoxide.

together with copper(II) phthalocyanine-3,4′,4″,4‴-tetrasulfonic acid, tetrasodium salt.[43] The IR spectrum presents the characteristic vibrational bands for phthalocyanine with in particular the ones of sulfonate; the interlayer distance is increased to 25.8 Å. This is in agreement with the copper phthalocyanine lying in the gallery parallel to the layers since its dimensions are evaluated to be $19.9 \times 17.3 \times 5.5$ Å^3.[50] The absorption spectrum (Fig. 10) indicates that in the material molecules form dimers since the Q band, peaking at 660 nm for the monomer species,[51] is shifted towards 600 nm. These preliminary results indicate than it is possible to graft or to insert relatively voluminous organic molecules in this system. Thus, the optically active species can be confined in the interlayer spacing.

In order to use these materials as bifunctional devices, it would be interesting to increase the paramagnetic-ferromagnetic transition temperature. Therefore, the possibility to reduce the divalent cation to the metallic state was explored,[40] since metal Ni is known to be ferromagnetic at room temperature with a Curie temperature close to 300 °C. One possibility is to anneal the sample under H_2. In order to optimise the reduction conditions, the magnetisation at 0.1 T was recorded under N_2 with 5% H_2 while heating the sample. At temperatures below 230 °C the signal is decreasing since the silicates are paramagnetic. Above this temperature, the signal increases, indicating the apparition of ferromagnetism in the sample. When observed by transmission electron microscopy, Ni metal nanoparticles were identified. In fact, further studies indicate that a reductive atmosphere is even not necessary to induce Ni^{2+} reduction. Annealing under purified Ar or under primary vacuum induces the formation of nanoparticles in the solid. Decomposition of acetate anions under an inert atmosphere leads to the formation of reductive species such as carbon monoxide in a first step. When the annealing time is increased, decomposition of the amino group takes place, also inducing reductive species and a second nucleation of nanoparticles can occur. Depending on the temperature and heating time, the size can be tuned but is in the range of 15–30 nm. Such particles are ferromagnetic with a coercive field close to 0.02 T. The originality of this approach is based on a low temperature annealing, which allows the coherence of the material to be kept when it is settled on different substrates. In particular, as long as the amino group is not decomposed, the film is adhesive on glass, MgO or mica. In this case, the functionality is still available. In Fig. 11(a) is reported a typical TEM picture of a reduced film cross section, together with an enlargement of a Ni metallic nanoparticle [Fig. 11(b)].

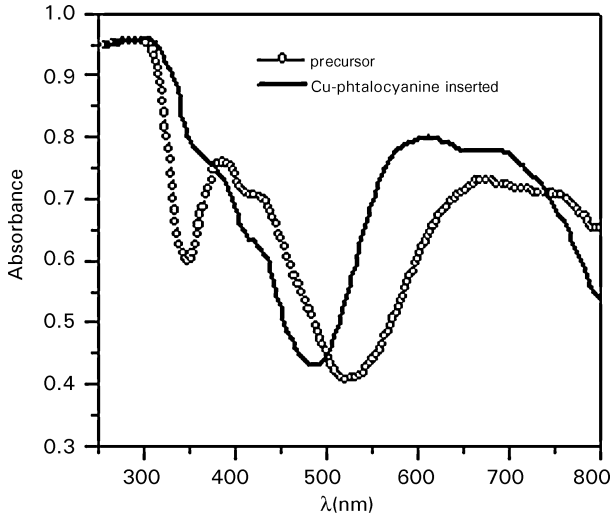

Fig. 10 UV spectrum of a Ni organic-inorganic phyllosilicate and the Cu phthalocyanine anion-exchanged one.

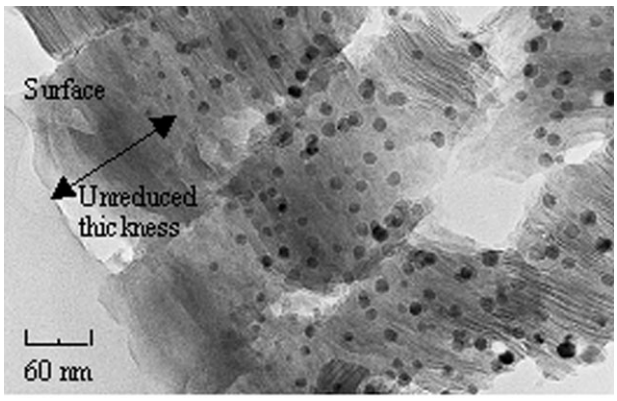

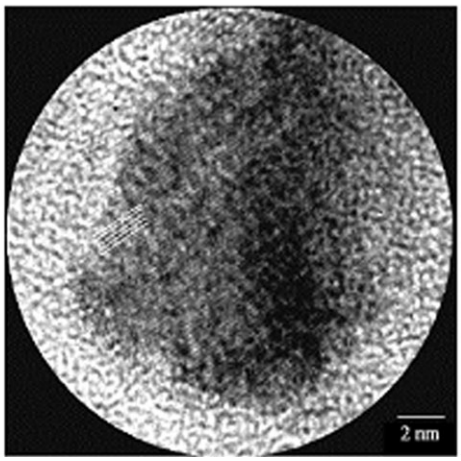

Fig. 11 Transmission electron microscopy images of (a) a cross section obtained by ultramicrotomy from an oriented film, reduced at 200 °C for 0.5 h under Ar; (b) enlargement of a Ni metallic nanoparticle; planes corresponding to 2 Å distance, indexed as (111) in the cubic cell of Ni metal, are visible.

Perspectives

Several features can be pointed out concerning these materials. It is expected that immobilisation of molecules with optical properties, for instance, will give rise to an enhanced response. In the case of Cu phthalocyanine, the Q band absorption can be tuned when low-concentration silica composites are obtained.[51] Concerning this particular molecule, it has already been shown that its catalytic property is greatly improved when it is introduced into an inorganic matrix.[52] It could thus be interesting to finely control the ion exchange rate by limiting the amount of Cu phthalocyanine reacted with the silicate suspension and decreasing the time of the reaction. Testing the accessibility of the amino group in the reduced solid could lead to promising materials. Certainly, original properties are to be expected with specific shaping of the studied samples, such as films obtained by settling.

However, complete physical comprehension can only be carried out if crystallisation is improved; this will be a very important challenge if we are to use these compounds as multi-property materials. In order to increase crystallinity, it appears important to better understand the growth mechanism of these materials. Especially, an effort is necessary to control the species present in the first step of the synthesis. In particular, it seems to be very important to finely understand the equilibrium involved during the formation of the layers. When introducing the alkoxide in an alcohol–water solution into the divalent cation solution, no real control over the species is performed. For instance, the tendency to form oligomers when organo-modified alkoxides are diluted in water–alcohol solution has been reported.[53] In particular, a stable octamer, $RSiO_{3/2}$, can

be formed and this species is allowed to react with the divalent cation solution. Even if smaller groups (monomers, dimers) can also remain in the solution, depending on its aging, hydrolysis of organically modified alkoxides especially is very rapid. Furthermore, condensation is self catalysed when dealing with the amino group. This means that before contacting both solutions, chemistry has probably already begun on the silicon side. This could explain why, depending on the modifier organic groups, condensation between Si atoms is different. Interesting materials could be synthesised starting from condensed organo-modified alkoxides such as has been obtained by treating 3-aminopropyltriethoxysilane with hydrochloric acid.[54] In this solid, hydrolysis and condensation are already achieved and the poly(3-aminopropyl)siloxane hydrochloride is a lamellar material in which chloride anions can be exchanged.

Acknowledgements

The authors are grateful to Agnès Traverse (LURE, Orsay) for XAS experimental facilities and her patient advice during fitting and Daniel Chateigner (ISMRA, Caen) for texture measurements on the orientated samples. Colleagues of the IPCMS are thanked for their contributions: Gaby Ehret (ultramicrotomy), Claude Estournes (nanoparticles), Jean-François Nierengarten (organic reactants) and Mohamedally Kurmoo for fruitful scientific discussions and polishing of the manuscript. Jean-Charles Ricquier (Institut des Matériaux Jean Rouxel) is also thanked for designing the cover picture.

References

1 P. Day, M. Kurmoo, T. Mallah, I. R. Marsden, R. H. Friend, F. L. Pratt, W. Hayes, D. Chasseau, J. Gaultier, G. Bravic and L. Ducasse, *J. Am. Chem. Soc.*, 1992, **114**, 10 722–10 729.
2 M. Kurmoo, A. W. Graham, P. Day, S. J. Coles, M. B. Hursthouse, J. L. Caulfield, J. Singleton, F. L. Pratt, W. Hayes, L. Ducasse and P. Guionneau, *J. Am. Chem. Soc.*, 1995, **117**, 12 209–12 217.
3 E. Coronado, J. R. Galán-Mascarós and C. J. Gómez-García, *Mol. Cryst. Liq. Cryst.*, 1999, **334**, 679–691; E. Coronado, J. R. Galán-Mascarós, C. J. Gómez-García and V. Laukhin, *Nature (London)*, 2000, **408**, 407–409.
4 Z. Gu, O. Sato, T. Iyoda, K. Hashimoto and A. Fujishima, *Mol. Cryst. Liq. Cryst.*, 1996, **286**, 469–474; S. Bénard, P. Yu, T. Coradin, E. Rivière, K. Nakatani and R. Clément, *Adv. Mater.*, 1997, **9**, 981–984.
5 P. G. Lacroix, R. Clément, K. Nakatani, J. Zyss and L. Ledoux, *Science*, 1994, **263**, 658–660.
6 P. C. LeBaron, Z. Wang and T. J. Pinnavaia, *Appl. Clay Sci.*, 1999, **15**, 11–29.
7 Y. Hotta, M. Taniguchi, K. Inukai and A. Yamagishi, *Langmuir*, 1996, **12**, 5195–5201.
8 P. Kannan, K. Pitchumani, S. Rajagopal and C. Srinivasan, *Chem. Commun.*, 1996, **3**, 369–370.
9 L. Coche-Guerente, V. Desprez and P. J. Labbe, *Electroanal. Chem.*, 1998, **458**, 73–86.
10 A. Szabo, D. Gournis, M. A. Karakassides and D. Petridis, *Chem. Mater.*, 1998, **10**, 369–645.
11 Y. Fukushima and M. Tani, *J. Chem. Soc., Chem. Commun.*, 1995, 241–242.
12 Y. Fukushima and M. Tani, *Bull. Chem. Soc. Jpn.*, 1996, **69**, 3667–3671.
13 Y. Hong and S. Kim, *Bull. Korean Chem. Soc.*, 1997, **18**, 236–238.
14 L. Ukrainczyk, R. A. Bellman and A. B. Anderson, *J. Phys. Chem. B*, 1997, **101**, 531–539.
15 S. Burkett, A. Press and S. Mann, *Chem. Mater.*, 1997, **9**, 1071–1073.
16 N. Whilton, S. Burkett and S. Mann, *J. Mater. Chem.*, 1998, **8**, 1927–1932.
17 M. da Fonseca, C. R. Silva, J. S. Barone and C. Airoldi, *J. Mater. Chem.*, 2000, **10**, 789–795.
18 M. da Fonseca and C. Airoldi, *J. Chem. Soc., Dalton Trans.*, 1999, 3687–3692.
19 V. Laget, *Thèse de Doctorat*, Université Louis Pasteur, Strasbourg, France, 1996; P. Rabu and M. Drillon, *Adv. Eng. Mater.*, 2003, **5**, 189–210.
20 S. W. Bailey, in *Reviews in mineralogy, Hydrous Phyllosilicates*, ed. P. H. Ribbe, Mineralogical Society of America, Washington, 1988, **vol. 19**.
21 B. Perdikatsis and H. Burzlaff, *Z. Kristallogr.*, 1981, **156**, 177–186.
22 (*a*) L. Huve, J. Baron, D. Saehr, R. Le Dred, in *Clays Controlling the Environment, Proceedings of the International Clay Conference*, ed. J. G. Churchman, R. W. Fitzpatrick and R. A. Eggleton, Commonwealth Scientific and Industrial Research Organization, East Melbourne, Australia, 1995, 243–248; (*b*) F. Lhommede, R. Le Dred, D. Saehr and J. Baron, *C. R. Acad. Sci., Ser. IIa: Sci. Terre Planetes*, 1996, **322**, 827–830; (*c*) J. T. Kloprogge, S. Komarneni and J. E. Amonette, *Clays Clay Miner.*, 1999, **47**, 529–554.
23 M. Richard-Plouet and S. Vilminot, *Solid State Sci.*, 1999, **1**, 381–393.
24 M. Richard-Plouet and S. Vilminot, *J. Mater. Chem.*, 1998, **8**, 131–137.
25 M. Guillot, M. Richard-Plouet and S. Vilminot, *J. Mater. Chem.*, 2002, **12**, 851–857.
26 R. E. Schaak and T. E. Mallouk, *Chem. Mater.*, 2000, **12**, 2513–2516.
27 M. Richard-Plouet and S. Vilminot, unpublished results.
28 J. B. Goodenough, *Magnetism and the Chemical Bond*, John Wiley and Sons, New York, 1963.
29 M. da Fonseca, C. Silva and C. Airoldi, *Langmuir*, 1999, **15**, 5048–5055.
30 M. da Fonseca and C. Airoldi, *Thermochim. Acta*, 2000, **359**, 1–9.
31 M. da Fonseca and C. Airoldi, *J. Mater. Chem.*, 2000, **10**, 1457–1463.
32 I. L. Lagadic, M. K. Mitchell and B. D. Payne, *Environ. Sci. Technol.*, 2001, **35**, 984–990.
33 K. A. Carrado, L. Xu, R. Csencsits and J. V. Muntean, *Chem. Mater.*, 2001, **13**, 3766–3773.
34 C. R. Silva, M. G. Fonseca, J. S. Barone and C. Airoldi, *Chem. Mater.*, 2002, **14**, 175–179.
35 B. Lebeau, N. T. Whilton and S. Mann, *Mater. Res. Soc. Symp.*, 2002, **726**, 27–32.
36 M. Jaber, J. Miehe-Brendle, M. Roux, J. Dentzer, R. Le Dred and J.-L. Guth, *New J. Chem.*, 2002, **26**, 1597–1600.
37 M. Jaber, J. Miéhé-Brendlé, L. Delmotte and R. Le Dred, *Microporous Mesoporous Mater.*, 2003, 155–163.
38 K. Fujii, S. Hayashi and H. Kodama, *Chem. Mater.*, 2003, **15**, 1189–1197.
39 E. P. Plueddemann, *Silane Coupling Agents*, Plenum Press, New York, 1982; C. Chiang, H. Ishida and J. L. Koenig, *J. Colloid Interface Sci.*, 1980, **74**, 396.
40 M. Guillot, *Thèse de Doctorat*, Université Louis Pasteur , Strasbourg, France, 2002.
41 M. G. Voronkov and V. I. Lavrent'yev, *Top. Curr. Chem.*, 1982, 102–199.
42 A. Walcarius, M. Etienne and J. Bessière, *Chem. Mater.*, 2002, **14**, 2757–2766.
43 M. Richard-Plouet, S. Vilminot, M. Guillot and M. Kurmoo, *Chem. Mater.*, 2002, **14**, 3829–3836.
44 M. Richard-Plouet, M. Guillot, A. Traverse, D. Chateigner and S. Vilminot, *Nucl. Instrum. Methods Phys. Res., Sect. B*, 2003, **200**, 148–154.
45 (*a*) A. Manceau, D. Chateigner and W. P. Gates, *Phys. Chem. Min.*, 1998, **25**, 347–365; (*b*) M. Schlegel, A. Manceau, D. Chateigner and L. Charlet, *J. Colloid. Interface Sci.*, 1999, **215**, 140–158; (*c*) M. Schlegel, *Thèse de Doctorat*, Université Joseph Fourier, Grenoble I, Grenoble, France, 2000; (*d*) A. Manceau, B. Lanson, V. A. Drits, D. Chateigner, W. P. Gates, J. Wu, D. Huo and J. W. Stucki, *Am. Mineral.*, 2000, **85**, 133–152.
46 S. M. Heald and E. A. Stern, *Phys. Rev. B*, 1977, **16**, 5549–5559.
47 J. Dittmer and H. Dau, *J. Phys. Chem. B*, 1998, **102**, 8196–8200.
48 A. Manceau and M. Schlegel, *Phys. Chem. Miner.*, 2001, **28**, 52–56.
49 X. Zhang, X. You, S. Ma and Y. Wei, *J. Mater. Chem.*, 1995, **5**, 643–647.
50 K. A. Carrado, J. E. Forman, R. E. Botto and R. E. Winans, *Chem. Mater.*, 1993, **5**, 472–478.
51 P. D. Fuqua, B. Dunn and J. I. Zink, *J. Sol-gel Sci. Technol.*, 1998, **11**, 241–250.
52 S. Kannan, S. V. Awate and M. SM Agashe, *Recent Adv. Basic Appl. Aspects Ind. Catal. (Stud. Surf. Sci. Catal.)*, 1998, **113**, 927–935.
53 J. Rozière, D. Jones and T. Cassagneau, *J. Mater. Chem.*, 1991, **1**, 1081–1082; K. Piana and U. Schubert, *Chem. Mater.*, 1995, **7**, 1932–1937.
54 Y. Kaneko, N. Iyi, T. Matsumoto, K. Fujii, K. Kurashima and T. Fujita, *J. Mater. Chem.*, 2003, **13**, 2058–2060.